



Preparation of all-cellulose composites with optical transparency using the banana pseudostem as a raw material

L. Chávez-Guerrero · S. Vazquez-Rodriguez · J. A. Salinas-Montelongo ·
L. E. Roman-Quirino · N. A. García-Gómez

Received: 19 October 2018 / Accepted: 7 March 2019 / Published online: 14 March 2019
© Springer Nature B.V. 2019

Abstract Biopolymers are intended to substitute the petroleum-based polymers and all-cellulose composite has emerged as a green alternative, especially if it can be prepared through a method consuming less energy and fewer chemicals. Here, a novel approach to obtain a nanocomposite film made of cellulose fibrils imbibed into a nanocellulose matrix is described. Banana pseudostem was used as raw material and characterized along with the resulting materials using scanning electron microscopy, optical microscopy and Raman spectroscopy, while the cellulose/nanocellulose film was studied through X-ray diffraction, UV–

Vis-NIR spectroscopy and laser scanning microscopy. Results indicate that cellulose (fibrils) and nanocellulose (platelets), extracted from banana pseudostem were successfully purified using hydrolysis at a relatively low amount of chemicals. Transparent films made of a fibrils/nanoplatelets blend were prepared by the solution casting method, exhibiting a transmittance of ≈ 83 – 88% and a crystallinity index of ≈ 70 , hence demonstrating the feasibility of this novel method to obtain cellulose/nanocellulose free-standing films.

L. Chávez-Guerrero · S. Vazquez-Rodriguez ·
J. A. Salinas-Montelongo
Facultad de Ingeniería Mecánica y Eléctrica, Universidad
Autónoma de Nuevo León, Pedro de Alba s/n,
66451 San Nicolás de los Garza, Nuevo León, México

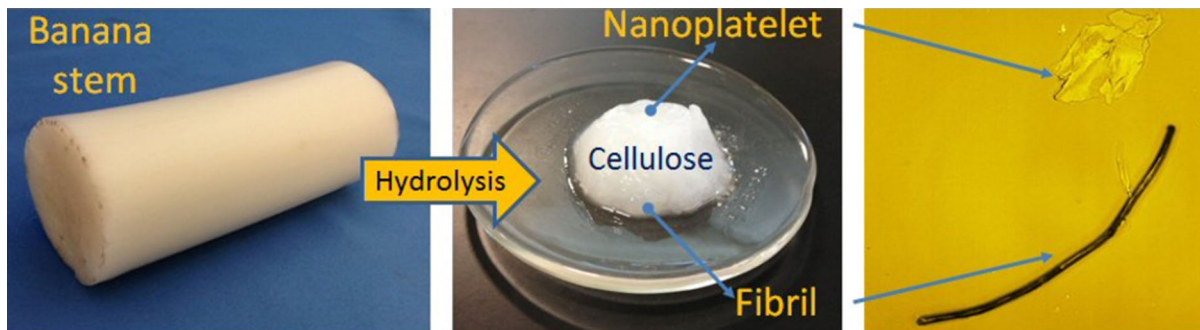
L. Chávez-Guerrero (✉) · S. Vazquez-Rodriguez
Centro de Innovación, Investigación y Desarrollo en
Ingeniería, Universidad Autónoma de Nuevo León
UANL, Av. Alianza 101 Sur Km. 10 de la Nueva
Carretera Internacional de Monterrey,
C.P. 66600 San Nicolás de los Garza, Nuevo León,
Mexico
e-mail: leonardo.chavezgr@uanl.edu.mx

L. E. Roman-Quirino
Universidad Politécnica de Apodaca, Av. Politécnica cruz
con la Carretera Miguel Alemán, Km 24.5,
C.P. 66600 Apodaca, NL, México

N. A. García-Gómez
Facultad de Ciencias Químicas, Universidad Autónoma
de Nuevo León, Ave. Universidad s/n, Ciudad
Universitaria, C.P. 66451 San Nicolás de los Garza,
Nuevo Leon, Mexico

N. A. García-Gómez
Centro de Investigación en Biotecnología y
Nanotecnología (CIByN). Facultad de Ciencias Químicas,
Universidad Autónoma de Nuevo León (UANL). Parque
de Investigación e Innovación Tecnológica,
66629 Apodaca, Nuevo León, México

Graphical abstract



Keywords Cellulose/nanocellulose films · Agricultural waste · Cellulose nanoplatelets · Inner pseudostem · Nanocomposites

Abbreviations

BI-Ctrl	Control sample
BI-Alk	Sample under alkaline pretreatment
BI-Hyd	Sample under acidic pretreatment
BP	Sample under basic pretreatment
CNP	Cellulose nanoplatelets
CrI	Crystallinity index
XRD	X-ray diffraction
OM	Optic microscopy
SEM	Scanning electron microscopy
LSM	Laser scanning microscopy

Introduction

Recently, all-cellulose composites conformed of fibrils imbibed into a matrix become an interesting option as biopolymer composites, since they are biodegradable and considered environment-friendly materials (Nishino et al. 2004; Dufresne 2013; Chávez-Guerrero et al. 2017). Most composites are integrated of at least two components, which are chemically different, creating an interface between the matrix and the reinforcement, which is usually a fiber. Some challenges duo to interface problems is poor adhesion, bad fiber distribution, and moisture uptake by the composites. To overcome these problems, the fiber and matrix could be composed of the same polymer, achieving compatibility, recyclability, and good

interfacial adhesion (Nishino et al. 2004; Yang and Berglund 2018).

Cellulose is biosynthesized by land plants through photosynthesis, is made of glucose molecules which in turn are formed from water and carbon monoxide (Ivakov et al. 2017). Converting light energy into chemical energy using CO₂ as a source of carbon is of great advantage (Ivakov et al. 2017), especially when glucose in the form of nanocellulose can be stored in the cell wall. The petroleum based polymers have a huge demand (Ferrer et al. 2017), which cannot be covered at the moment by degradable biopolymers (Adeodato Vieira et al. 2011), then a better process and more suitable raw materials (biomass) must be studied and developed (Chávez-Guerrero et al. 2017, 2018; Dufresne 2013). Nanocellulose is one outstanding product that can be obtained from residual biomass, having low density, biodegradability, high aspect ratio, great mechanical and chemical resistance, and abundance (Dufresne 2013). Since cellulose is the most abundant biopolymer on earth (Espino et al. 2014), it is reasonable to intend to take advantage of this huge renewable source, where micro and nanomaterials can be isolated from biomass. Banana production occurs worldwide, mainly in tropical countries, with only some varieties been exploited regardless of the 1200 available, sharing a common characteristic (Aurore et al. 2009), all are perennial plants that are disposed of once the fruit is collected (single harvest), which can lead to an environmental problem, if the residual biomass at the plantations is not appropriately managed. The fruit is only 12% of the total mass (Zuluaga et al. 2007); the rest consists of leaves, rachis, peels, stalk, inflorescence, stem and the pseudostem (Padam et al. 2014). The pseudostem has a soft fiber in the innermost (stem) and coarse fiber

at the outer section, which has been used mainly in the textile industry. Over 117 million tons of banana fruit were produced in 2015 (Banana market Review 2015), mainly produced in Asia, Africa and Latin America. Several ways to isolate nanocellulose using banana pseudostem have been proposed. The approaches include three general steps, which are: (1) pretreatment of the raw material, (2) hydrolysis assisted by concentrated acids (60–65%) (Mueller et al. 2014), with a posterior (3) defibrillation by TEMPO/ultrasonication (Faradilla et al. 2016; Khawas and Deka 2016), mechanical milling (Phanthong et al. 2017; Tibolla et al. 2018), steam explosion (Cherian et al. 2008; Deepa et al. 2011, 2015) or enzymatic treatment (Tibolla et al. 2018). All of the processes reported (in our best knowledge), require several steps (some steps were done twice) to obtain the cellulose or nanocellulose from banana pseudostem (and most raw materials), in consequence having a high consumption of energy, chemicals and time. This paper aims to introduce a novel process using the banana stem as a raw material under alkaline peroxide treatment, followed by hydrolysis using a low amount of acid (2% v/v), hence producing an all-cellulose nanocomposite.

Materials and methods

Materials

The chemicals used were H_2O_2 , NaOH, H_2SO_4 , and methylene blue, were analytical grade reagent and used without any further purification. The raw material was obtained from the state of Nuevo Leon in Mexico. The inner banana pseudostem (*Musa sapientum*) was collected after harvest, then cut into pieces of about $0.5 \times 3 \times 10$ cm (thickness \times width \times length).

Mechanical separation

The banana stem samples were stored inside plastic bags and frozen at -50 °C for 12 h, then freeze-dried for 48 h until 80% of the water was extracted. Dried samples were milled on a Bel Art 37250 Micro-Mill Grinder for 30 s. The resultant powder was passed through a #150 sieve, then used as a control and named *BI-ctrl* thereafter.

Cellulose extraction

Five grams of the sample *BI-ctrl* were placed on a conical flask containing 80 mL of deionized water, 20 mL of H_2O_2 (20% v/v) and 2 g of NaOH (2% w/v), kept it under constant stirring at 100 rpm at 60 °C for 60 min to achieve the alkaline/bleaching procedure, this sample was named *BI-Alk* thereafter. The dispersion was separated by filtration and washed with deionized water two times; then H_2SO_4 was added drop by drop to neutralize the suspension (pH 7) and washed one more time. The hydrolysis was carried on using 88 mL of deionized water with 10 mL of H_2O_2 (10% v/v) and 2 mL of H_2SO_4 (2% v/v). After that, 10 g of the sample *BI-Alk* was added to the solution, kept it under constant stirring at 100 rpm for 10 min, and then the dispersion was placed inside an autoclave at 110 °C for 40 min. When the time lapsed, the autoclave was turn off and opened once the internal temperature reached 80 °C. The dispersion was separated by filtration and washed with deionized water two times; then sodium hydroxide pellets were added to neutralize the suspension (pH 7) and washed two more times with deionized water. The resulting gel (10% w/v) was labeled *BI-Hyd* thereafter. Using this gel, which is a pulp rich in CNPs and cellulose fibrils (*BI-Hyd*), free-standing films were produced by the solution casting method on a Petri dish, then drying the film in an oven at 40 °C for 5 h.

Micro Raman spectroscopy

Raman spectra were acquired using a Thermo Scientific DXR Raman spectrometer coupled to an optic microscope. The wavelength to excite the sample was 532 nm at room temperature, and a resolution of 4 cm^{-1} . The measurements were recorded in a wavenumber range from 250 to 1800 cm^{-1} . A drop of each sample was dried on glass microscope slide in an oven at 40 °C for 3 h. The spectral data were scanned for the acquisition of up to 5 accumulations and 5 s exposure.

Optic microscope (OM)

A Leica light microscope DM 3000 model was used to observe all samples at different scales. To enhance the contrast between the glass and the samples, a methylene blue solution of 0.1% (w/v) was used. A

drop of each sample was deposited on a glass microscope slide, and then it was dried at 40 °C for 2 h. Then, a drop of the methylene blue solution was deposited on each sample for 30 s, then it was rinsed with distilled water three times; finally, it was dried at 40 °C for 2 h.

Scanning electron microscope (SEM)

The samples were analyzed in a scanning electron microscope FEI Nova NanoSEM 200, under high vacuum with a secondary electron detector (ETD). The microscope was operated at 5–10 kV, and working distance of 5 mm. The samples were dispersed in ethanol, and then a drop of every sample was dried on silicon wafers at 40 °C for 2 h. The silicon wafers were glued to an aluminum pin and observed without a conductive coating.

Laser scanning microscope (LSM)

In order to obtain height profiles of the particles inside the *BI-Hyd* sample, a ZEISS LSM 700 laser scanning microscope (LSM) with a laser emitting at 405 nm was used. A drop of the sample dispersion was deposited on a silicon wafer and dried at 40 °C for 2 h, and then the silicon wafer was glued to a glass microscope slide. All images were acquired with the 100× lens, using 512 × 512 pixels and 150 layers to build each image.

UV–Vis–NIR spectrometer

The characterization of the optical properties was performed using an Agilent Cary 5000 UV–Vis–NIR spectrometer, equipped with an integrating sphere with scatter transmission port and air as base line. The percent transmittance and absorbance spectra were acquired in the wavelength range of 400–800 nm at a scan rate of 400 nm/min. The transparency (T) of the films was calculated following the equation: $T = A_{550\text{nm}}/x$, where A is absorbance value at 550 nm and x is the film thickness in mm (Bao et al. 2009).

X-ray diffraction analysis (XRD)

The samples were analyzed by X-ray diffraction, in a D8 Advance Bruker powder diffractometer at room

temperature. A Cu-K α ($\lambda = 1.5406 \text{ \AA}$) radiation was used to collect the diffraction patterns within Bragg angle 2θ from 5° to 40°, using a step of 0.05° and a time step of 1 s. The crystallinity index CrI was calculated using the Eq. (1). The crystallinity index (CrI) was calculated following the Eq. (1), where I_{total} indicates the maximum intensity at the plane 200 and I_{am} the minimum diffraction intensity at $\approx 18^\circ$, which represents the amorphous contribution (Segal et al. 1959).

$$CrI(\%) = \frac{I_{\text{total}} - I_{\text{am}}}{I_{\text{total}}} \times 100 \quad (1)$$

Results and discussion

Pretreatment process

Figure 1 shows the appearance of the involved materials during the production of all-cellulose composites. Figure 1a shows the characteristics of the banana inner stem, having a 3 cm in diameter and 12 cm long. Once the material was freeze-dried (Fig. 1b) and milled, the obtained powder became darker, which is shown in Fig. 1c. The powder under alkaline treatment become bright green/yellow (Fig. 1d) and some of the lignin was extracted under that procedure. Then, after the hydrolysis, the lignin and inorganic crystals were totally removed, also the bleaching was completed (Fig. 1e).

Micro Raman spectroscopy

The dactyloscopic region of cellulose in the Raman spectra (300–1700 cm^{-1}), provides a chemical insight into what occurs to the sample after each step, as seen in Fig. 2. The peaks at 1265 cm^{-1} , 1607 cm^{-1} and 1635 cm^{-1} corresponding to lignin (Gierlinger et al. 2012) are clearly visible in the case of *BI-Ctrl*. Nevertheless their intensities are shielding other important peaks of cellulose. The peak at 1173 cm^{-1} in the raw sample spectrum is related to the hydroxycinnamic acid, also found and reported in *Miscanthus sinensis* (Ma et al. 2014). After the alkaline treatment (*BI-Alk*), the lignin peaks were reduced but not eliminated, allowing evaluating the grade of purification at every step of the process. The characteristic peaks of cellulose at 1095 cm^{-1} , 1020 cm^{-1} ,

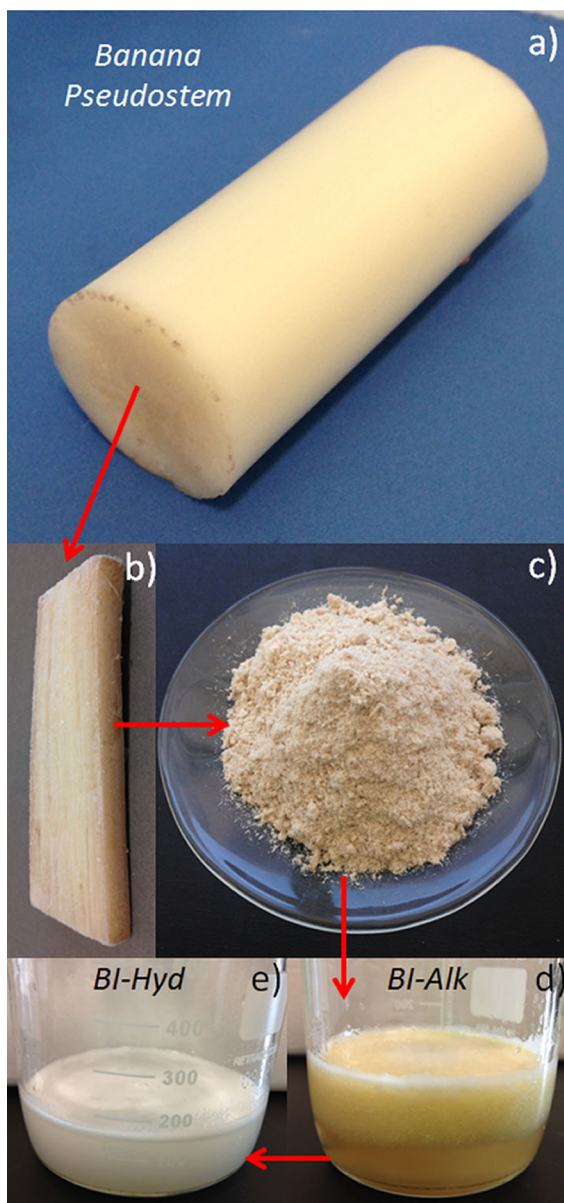


Fig. 1 Digital photographs of the samples on each step of the procedure. The raw banana stem in (a), the lyophilized sample in (b), the milled powder in (c), while the alkaline and acid treatment are shown in (d) and (e) respectively

898 cm^{-1} , and 380 cm^{-1} were revealed in the spectrum of the *BI-Alk* sample after the bleaching/alkaline treatment, coexisting with the ones of lignin, suggesting a partial delignification (Gierlinger et al. 2012). Once the hydrolysis is performed (*BI-Hyd*), the lignin is solubilized and most contaminants eliminated (pectin, proteins, salts), then the cellulose backbone

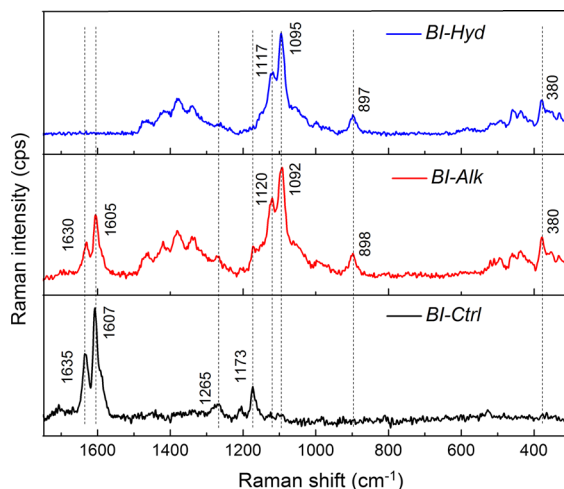


Fig. 2 Raman spectra showing the processes effect on the biomass components

appears, corroborating a proper cellulose isolation. Similar results were previously reported, when *Agave salmiana* leaves were subjected to a low concentration of H_2SO_4 in presence of H_2O_2 , showing that nanocellulose can be obtained from the parenchyma of different plants (Chávez-Guerrero et al. 2017).

The spectrum corresponding to *BI-Hyd* indicates the absence of lignin and other organic and inorganic compounds, which shows that the hydrolysis procedure, consisting only of 2% v/v of H_2SO_4 assisted by H_2O_2 , was enough to remove the remaining impurities from the previously bleached material.

Microscopy analysis (OM, SEM, LSM)

The images obtained with the optic microscope (OM) indicated the presence of phenolic groups, in a qualitative way, because methylene blue is used to detect pectin and lignin (Vermerris and Nicholson 2008), allowing to understand the effect of the different chemical treatments on the samples. As shown in Fig. 3a, the fibers and cell walls developed a dark blue color, which suggest the presence of lignin at the surface. However, after the alkaline treatment was performed, the intensity of the color clearly decreased, as seen in Fig. 3c. After the hydrolysis, the fibers become loose (inset in Fig. 3e), presumably because of the effect of the acid on the amorphous cellulose, which may cause the breaking of the fiber continuity, producing shorter fibers with no lignin on their surface

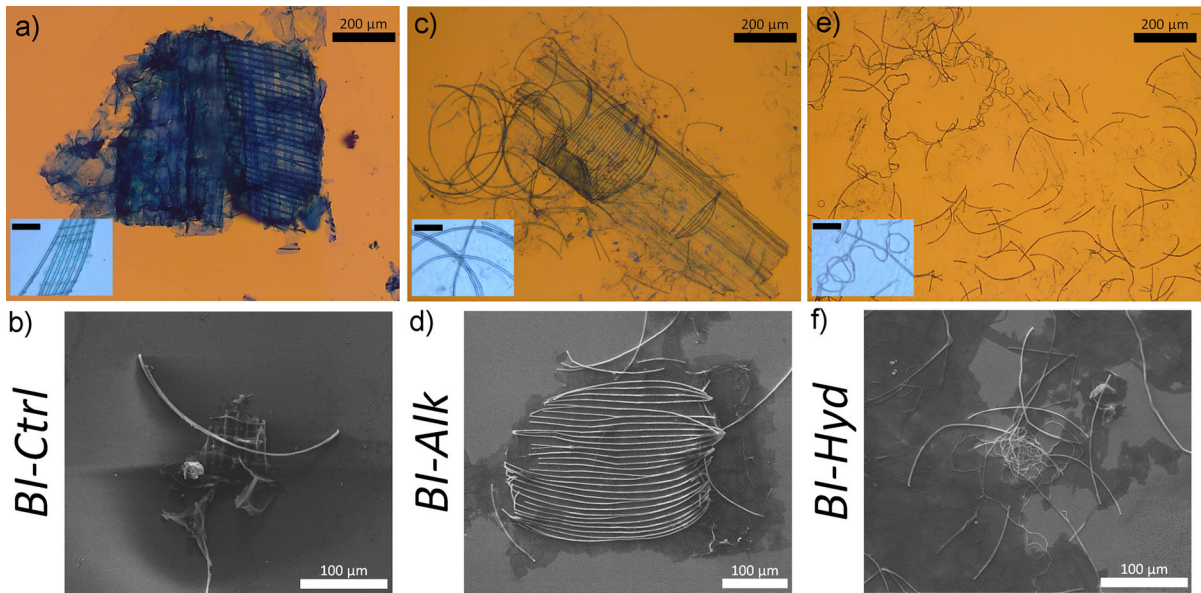


Fig. 3 Images from the OM and SEM corresponding to BI-Ctrl in (a, b), BI-Alk in (c, d) and BI-Hyd in (e, f). The scale in the inset for (a, c, e) is 50 μm

(Fig. 3e–f). SEM images also help to elucidate that the fibers have cylindrical shape with a diameter of $\approx 2.5 \pm 0.3 \mu\text{m}$, the measurements were done after the hydrolysis process (BI-Hyd). As seen in Fig. 3a, spiral structures were present in the raw material (BI-

Ctrl), however, the fibers appeared broken after the alkaline treatment (BI-Alk). Similar results were reported by Gañán et al. (2008), where the hierarchical arrangements of the fibrous structures, named conducting tissue, were presented.

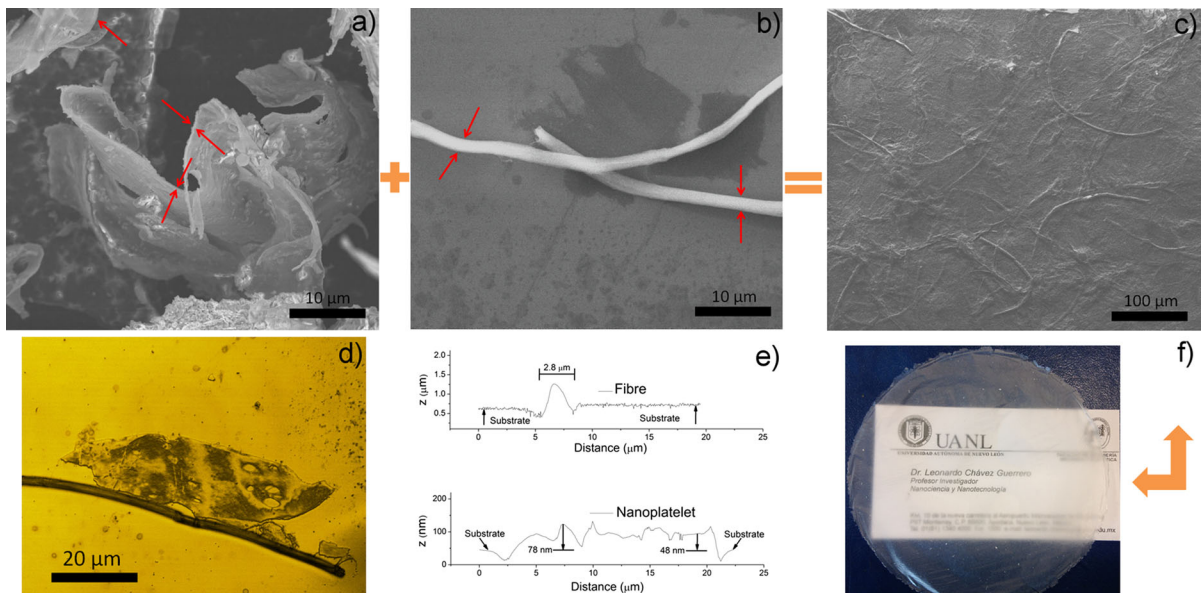


Fig. 4 SEM images of the raw material containing parenchyma and fibers, shown in (a) and (b) respectively. LSM image showing the laminar/fiber structures in (d) and height profiles of

those structures in (e). A SEM image and a digital photo of the film are shown in (c) and (f) respectively

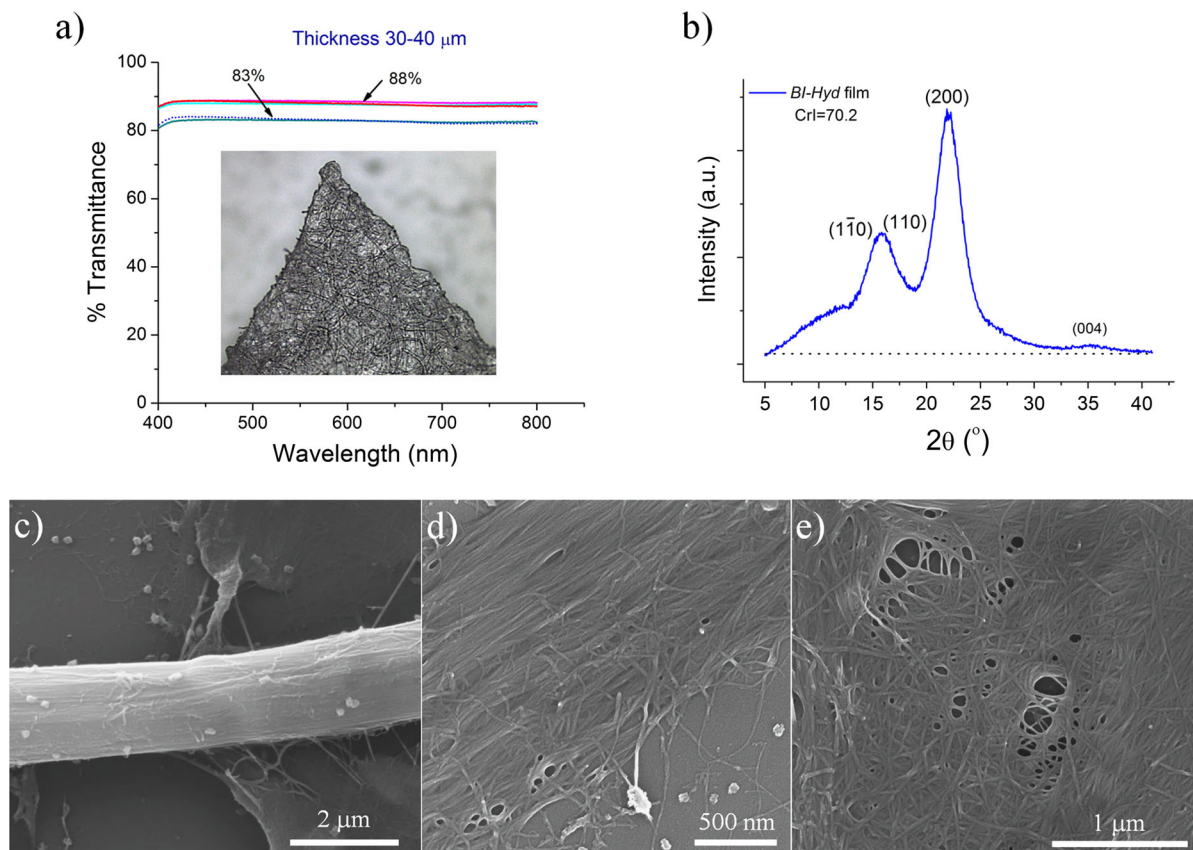


Fig. 5 The nanocellulose film transmittance is shown in (a). XRD results are shown in (b) indicating the crystallinity and SEM images showing the nanofibrils inside the CNPs in (c–e)

The LSM results showed that the cellulose nanoplatelet (CNP) thickness has a maximum value of ≈ 78 nm (Fig. 4e), making it a nanostructure, which has a strong influence in the optical properties of the film, making it transparent (Fig. 4f). The good fiber distribution results in the absence of bundles, avoiding the light dispersion (Fig. 4c).

Due to CNPs have holes at different points, and the thickness is variable along the nanoplatelet (Fig. 4e), the thickness cannot be considered homogeneous, for this reason only the maximum height is reported (≈ 78 nm) to prove that the CNP is a nanoparticle (ISO 2015), which was previously reported by Chávez-Guerrero et al., in the case of *Agave salmiana* (Chávez-Guerrero et al. 2017).

The LSM images also exhibit the characteristics of both structures (Fig. 4d), which are the fibrils (Fig. 4b) and the CNPs (Fig. 4a), corresponding to the cellulose/nanocellulose components inside the film (Fig. 4c), both extracted from the banana

pseudostem. The interaction of both laminar and fibrous structures produces a free-standing/translucent film. The SEM images suggest that the lamellar nanostructures act as a matrix and plasticizer to keep embedded the fiber and give some flexibility to the film (Adeodato Vieira et al. 2011), since the CNP is at least 30 times thinner than the fiber (Fig. 4e).

Cellulose/nanocellulose isolation

The film made of CNPs/microfibrils showed 83–88% of transmittance (Fig. 5a) and the transparency value (T) was $2.5 (\pm 0.66)$ obtained from different zones of films with ≈ 30 – 40 μm thickness. As previously seen, Raman results indicate a proper lignin removal (Fig. 2), which is in accordance with the good transmittance presented by the composites. Those values, are comparable with films made entirely of nanocellulose ($\approx 80\%$ at 550 nm), or a blend of nanocellulose and synthetic polymers (Chen et al.

2014; Sun et al. 2018; Yang and Berglund 2018). It is important because the success of polymers e.g. used in packaging lies in the ability to display their interior (Ferrer et al. 2017). In the case of natural fibers, the thinner the fibers, the higher the quality of the fiber, which could give an insight of the properties of the banana pseudostem fiber when used as reinforcement (Ferrer et al. 2017). A good fiber dispersion can be seen in Fig. 4c, also appreciated in the inset of Fig. 5a, which corresponds to an image from the optic microscope coupled at the Raman spectrometer. Such observation was also supported by the good transmittance presented by the all-cellulose film, which overcomes the most common problem for composites, the inhomogeneous fiber distribution. However, more experiments and characterization have to be done in future works, to obtain the fiber distribution and the possible use of this material in e.g. packaging or transparent substrate. The Fig. 5e shows a hole in the middle of one CNP, which was previously seen in a LSM image (Fig. 4d), suggesting a selective solubilization of the amorphous material during the hydrolysis.

XRD diffractogram in Fig. 5b indicates a successful purification of the cellulose. The amorphous material has an important inference in the profile shape, which suggests a mix of a highly crystalline

material, such as the fiber, and a less crystalline structure, the CNPs. The characteristic peaks of cellulose can be observed at 15.1° (double) and 22.3° (French 2014), with a crystallinity index of $\text{CrI} = 70.2\%$. This result was accomplished due to the treatment effectiveness. A small peak around 35° is due to the parallel ordering of cellulose inside the fiber (French 2014), while the nanoplatelets do not contribute to the intensity of that peak. These results are in agreement with previous reports and Raman results, where cellulose nanoplatelets extracted from *Agave salmiana* were observed (Chávez-Guerrero et al. 2018).

Previous reports indicate the CNPs are composed of nanofibrils (Chávez-Guerrero et al. 2018), which are inherent to the plant cell wall (parenchyma), as it can be seen in Fig. 5c–e, which is also true in the case CNPs extracted from the banana stem. A schematic representation of a CNP and a microfibril is depicted in Fig. 6, nanofibrils at the border of the CNP can be seen, where most of the fibrils remain entangled, allowing a possible anchorage between CNPs or even with the microfibrils. Using the same material as matrix (nanocellulose) and reinforcement microfibril (cellulose), some great advantages such as better interaction and adhesion thorough hydrogen bonding and less weight can be expected (Nishino et al. 2004),

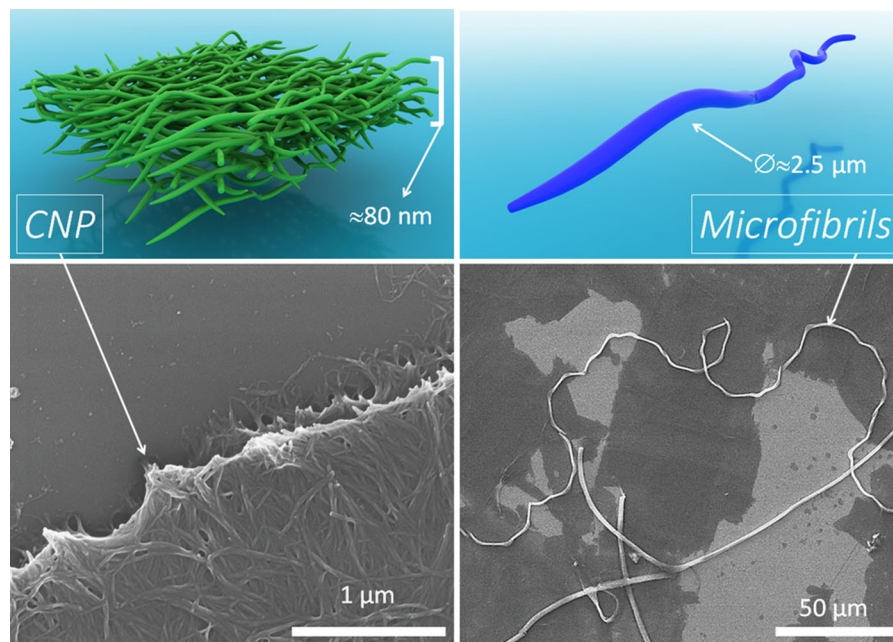


Fig. 6 Schematic representation of the all-cellulose components of the composites, CNP and microfibrils

suggesting a future trending in the production of biodegradable nanocomposites.

Also, Fig. 6 shows the appearance of a CNP once is purified, after the hydrolysis process, suggesting a proper elimination of lignin, as established by the XRD and RAMAN results. The two components inside the transparent films are made of cellulose (microfibril) and nanocellulose (CNP), purified at the same time from the inner banana pseudostem, which suggests potential advantages when used as an all-cellulose composite.

Conclusions

As stipulated in this novel method, less H_2SO_4 was required for the cellulose purification using the banana pseudostem, only 2%, compared to the usual 64%. Also, no need of treatment was required after hydrolysis to obtain the nanocellulose. Raman results unveiled a first stage of partial delignification and bleaching, and then the nanocellulose purification through hydrolysis was successfully conducted. Cellulose nanoplatelets (CNP) with a thickness of ≈ 78 nm and cellulose microfibrils of $\varnothing = 2.5 \pm 3$ μm were purified at the same time. An all-cellulose composite was produced using a combination of a nanocellulose matrix and cellulose fibrils, both extracted from the inner banana pseudostem. A free-standing film made of a cellulose/nanocellulose biopolymer, with ≈ 83 –88% transmittance and crystallinity index of 70.2 was successfully obtained.

References

- Adeodato Vieira MG, Altenhofen da Silva M, Oliveira dos Santos L, Beppu MM (2011) Natural-based plasticizers and biopolymer films: a review. *Eur Polym J* 47:254–263. <https://doi.org/10.1016/j.eurpolymj.2010.12.011>
- Aurore G, Parfait B, Fährsman L (2009) Bananas, raw materials for making processed food products. *Trends Food Sci Tech* 20:78–91. <https://doi.org/10.1016/j.tifs.2008.10.003>
- Banana market Review (2015–2016). Food and Agriculture Organization of the United Nations, Rome
- Bao S, Xu S, Wang Z (2009) Antioxidant activity and properties of gelatin films incorporated with tea polyphenol loaded chitosan nanoparticles. *J Sci Food Agric* 89:2692–2700. <https://doi.org/10.1002/jsfa.3775>
- Chávez-Guerrero L, Sepúlveda-Guzmán S, Rodríguez-Liñan C, Silva-Mendoza J, García-Gómez N, Pérez-Camacho O (2017) Isolation and characterization of cellulose nanoplatelets from the parenchyma cells of *Agave salmiana*. *Cellulose* 24:3741–3752. <https://doi.org/10.1007/s10570-017-1376-9>
- Chávez-Guerrero L, Sepúlveda-Guzmán S, Silva-Mendoza J, Aguilar-Flores C, Pérez-Camacho O (2018) Eco-friendly isolation of cellulose nanoplatelets through oxidation under mild conditions. *Carbohydr Polym* 181:642–649. <https://doi.org/10.1016/j.carbpol.2017.11.100>
- Chen G, Zhang B, Zhao J, Chen H (2014) Development and characterization of food packaging film from cellulose sulfate. *Food Hydrocoll* 35:476–483. <https://doi.org/10.1016/j.foodhyd.2013.07.003>
- Cherian BM, Pothan LA, Nguyen-Chung T, Mennig G, Kottaisamy M, Thomas S (2008) A novel method for the synthesis of cellulose nanofibril whiskers from banana fibers and characterization. *J Agric Food Chem* 56:5617–5627. <https://doi.org/10.1021/jf8003674>
- Deepa B, Abraham E, Mathew Cherian B, Bismarck A, Blaker JJ, Pothan LA, Lopes Leao A, Ferreira de Souza S, Kottaisamy M (2011) Structure, morphology and thermal characteristics of banana nano fibers obtained by steam explosion. *Bioresour Technol* 102:1988–1997. <https://doi.org/10.1016/j.biortech.2010.09.030>
- Deepa B, Abraham E, Cordeiro N, Mozetic M, Mathew AP, Oksman K, Faria M, Thomas S, Pothan LA (2015) Utilization of various lignocellulosic biomass for the production of nanocellulose: a comparative study. *Cellulose* 22:1075–1090. <https://doi.org/10.1007/s10570-015-0554-x>
- Dufresne A (2013) Nanocellulose: a new ageless bionanomaterial. *Mater Today* 16:220–227. <https://doi.org/10.1016/j.mattod.2013.06.004>
- Espino E, Cakir M, Domenek S, Román-Gutiérrez AD, Belgacem N, Bras J (2014) Isolation and characterization of cellulose nanocrystals from industrial by-products of *Agave tequilana* and barley. *Ind Crop Prod* 62:552–559. <https://doi.org/10.1016/j.indcrop.2014.09.017>
- Faradilla RHF, Lee G, Rawal A, Hutomo T, Stenzel MH, Arcot J (2016) Nanocellulose characteristics from the inner and outer layer of banana pseudo-stem prepared by TEMPO-mediated oxidation. *Cellulose* 23:3023–3037. <https://doi.org/10.1007/s10570-016-1025-8>
- Ferrer A, Pal L, Hubbe M (2017) Nanocellulose in packaging: Advances in barrier layer technologies. *Ind Crops Prod* 95:574–582. <https://doi.org/10.1016/j.indcrop.2016.11.012>
- French AD (2014) Idealized powder diffraction patterns for cellulose polymorphs. *Cellulose* 21:885–896. <https://doi.org/10.1007/s10570-013-0030-4>
- Gañán P, Zuluaga R, Cruz J, Vélez JM, Retegi A, Mondragon I (2008) Elucidation of the fibrous structure of Musaceae mature rachis. *Cellulose* 15:131–139. <https://doi.org/10.1007/s10570-007-9150-z>
- Gierlinger N, Keplinger T, Harrington M (2012) Imaging of plant cell walls by confocal Raman microscopy. *Nat Protoc* 7:1694–1708. <https://doi.org/10.1038/nprot.2012.092>

- International Organization for Standardization (ISO) (2015) ISO technical specifications ISO/TS 80004-2:2015, Nanotechnologies-Vocabulary—Part 2: nano-objects
- Ivakov A et al (2017) Cellulose synthesis and cell expansion are regulated by different mechanisms in growing arabidopsis Hypocotyls. *Plant Cell* 29:1305. <https://doi.org/10.1105/tpc.16.00782>
- Khawas P, Deka SC (2016) Isolation and characterization of cellulose nanofibers from culinary banana peel using high-intensity ultrasonication combined with chemical treatment. *Carbohydr Polym* 137:608–616. <https://doi.org/10.1016/j.carbpol.2015.11.020>
- Ma J, Zhou X, Ma J, Ji Z, Zhang X, Xu F (2014) Raman microspectroscopy imaging study on topochemical correlation between lignin and hydroxycinnamic acids in *Miscanthus sinensis*. *Microsc Microanal* 20:956–963. <https://doi.org/10.1017/S1431927614000658>
- Mueller S, Weder C, Foster EJ (2014) Isolation of cellulose nanocrystals from pseudostems of banana plants. *RSC Adv* 4:907–915. <https://doi.org/10.1039/c3ra46390g>
- Nishino T, Matsuda I, Hirao K (2004) All-Cellulose Composite. *Macromolecules* 37:7683–7687. <https://doi.org/10.1021/ma049300h>
- Padam BS, Tin HS, Chye FY, MI A (2014) Banana by-products: an under-utilized renewable food biomass with great potential. *J Food Sci Technol* 51:3527–3545. <https://doi.org/10.1007/s13197-012-0861-2>
- Phanthong P, Karnjanakom S, Reubroycharoen P, Hao X, Abudula A, Guan G (2017) A facile one-step way for extraction of nanocellulose with high yield by ball milling with ionic liquid. *Cellulose* 24:2083–2093. <https://doi.org/10.1007/s10570-017-1238-5>
- Segal L, Creely JJ, Martin AE Jr, Conrad CM (1959) An empirical method for estimating the degree of crystallinity of native cellulose using the X-ray diffractometer. *Text Res J* 29:786–794. <https://doi.org/10.1177/004051755902901003>
- Sun X, Wu Q, Zhang X, Ren S, Lei T, Li W, Xu G, Zhang Q (2018) Nanocellulose films with combined cellulose nanofibers and nanocrystals: tailored thermal, optical and mechanical properties. *Cellulose* 25:1103–1115. <https://doi.org/10.1007/s10570-017-1627-9>
- Tibolla H, Pelissari FM, Martins JT, Vicente AA, Menegalli FC (2018) Cellulose nanofibers produced from banana peel by chemical and mechanical treatments: characterization and cytotoxicity assessment. *Food Hydrocolloid* 75:192–201. <https://doi.org/10.1016/j.foodhyd.2017.08.027>
- Vermerris W, Nicholson R (2008) Phenolic compound biochemistry. Springer, Dordrecht
- Yang X, Berglund LA (2018) Water-based approach to high-strength all-cellulose material with optical transparency. *ACS Sustain Chem Eng* 6:501–510. <https://doi.org/10.1021/acssuschemeng.7b02755>
- Zuluaga R, Putaux J-L, Restrepo A, Mondragon I, Gañán P (2007) Cellulose microfibrils from banana farming residues: isolation and characterization. *Cellulose* 14:585–592. <https://doi.org/10.1007/s10570-007-9118-z>

Publisher's Note Springer Nature remains neutral with regard to jurisdictional claims in published maps and institutional affiliations.